

On the Use of the First Order Shear Deformation Models of Beams, Plates and Shells in Creep Lifetime Estimations

K. Naumenko

Numerical creep–damage life–time predictions of thinwalled structures are discussed with respect to the cross section assumptions used in engineering models of beams, plates and shells. The first part of the paper is devoted to the comparative numerical study of a pipe bend based on shell and solid type finite elements available in the ANSYS code. The second part demonstrates the possibilities and limitations of the first order shear deformation beam theory in connection with creep damage analysis. The results show that the beam and shell models provide a satisfactory accuracy of time dependent deformation and stress solutions for the von Mises stress controlled creep response. The dependence of the creep strain rate on the kind of the stress state induced by the damage evolution requires to refine through–the–thickness approximations of displacement and stress fields used in the first order shear deformation engineering models. The errors of the creep solution with the shell or beam model result in the underestimation of displacements and the wrong edge zone stress redistributions.

1 Introduction

Creep continuum damage material models and finite element techniques have become an efficient tool for long-term predictions in structures at elevated temperatures, Hayhurst (1994). The first step is the description of the material behaviour by a suitable constitutive model with internal state variables characterising hardening and damage processes. Based on the material science and continuum mechanics foundations various models are proposed including physically motivated state variables and considering stress state dependences. With the progress in the material description the question arises about the applicability of available engineering structural mechanics models and corresponding finite element implementations to the creep damage analysis. Thin-walled structures are usually studied using the models of beams, plates and shells, which are based on the through-the-thickness approximations of three-dimensional displacement and stress fields and have been originally developed within the theory of linear elasticity (e.g. Reissner, 1985; Altenbach et al., 1998). A number of investigations show that the classical Kirchhoff–Love and first order shear deformation shell theories can accurately predict the creep deformation and creep buckling of shells considering material models of primary and secondary creep (e.g. Betten et al., 1989; Miyazaki, 1987; Takezono and Fujoka, 1981; Naumenko, 1996). The introduction of damage requires to take into account non-classical effects in the material behaviour, e.g. different tertiary creep rates by tension and compression or anisotropic behaviour induced by damage. As demonstrated in Bodnar and Chrzanowski (1994) the effect of different damage rates in tension and compression induces nonsymmetrical through-the-thickness damage distributions in a plate in bending, whereas the analysis has been based on the first order shear deformation theory. In Altenbach et al. (1997) the necessity to include geometrically nonlinear terms considering moderate rotations is discussed. However, these works do not answer the question, whether the classical through-the-thickness approximations, e.g. linear axial displacement or parabolic transverse shear stress approximations provide accurate predictions if the damage evolution is taken into account. Although a number of higher order models of beams, plates and shells are proposed for elastic sandwich or laminate structures (e.g. Reddy et al., 1997; Reissner, 1985), little effort has been made in studies on applicability of these refined models to creep–damage problems.

The aim of this paper is to discuss the numerical creep–damage predictions in thinwalled beams, plates and shells with respect to the cross–section assumptions. Particularly we examine the first order shear deformation shell theory, which is mostly used in the Finite Element codes, with the creep continuum damage material model. The first part of the paper illustrates the results of the shell and solid finite element based creep–damage simulation of a thinwalled pipe bend. The results are compared for various types of boundary conditions considering and neglecting the stress state effect of damage evolution. In the second part we discuss first order shear deformation beam equations and demonstrate the possibilities and limitations of the corresponding through-the-thickness approximations. Based on the Ritz method the simplified creep analysis of a beam is performed and compared with plane stress finite element simulation.

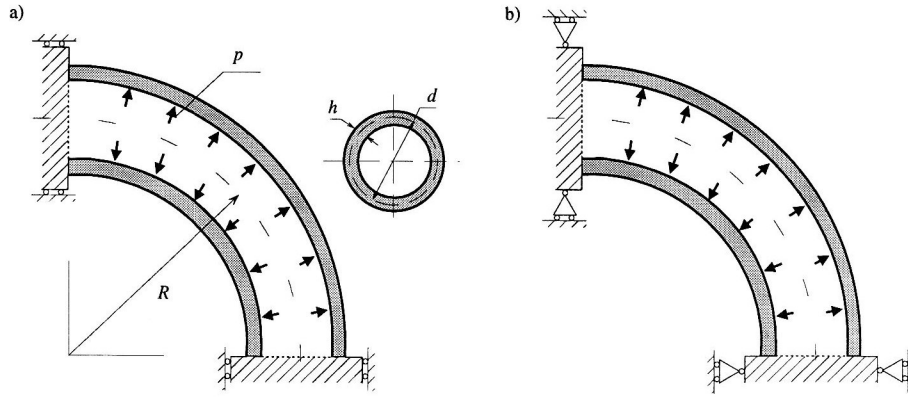


Figure 1. Pipe Bend Under Uniform Pressure, a) Boundary Conditions of Type I, b) Boundary Conditions of Type II

2 Finite Element Study of a Pipe Bend

Figure 1 shows a pipe bend loaded by internal pressure. The calculations have been performed with $R = 380$ mm, $d = 152$ mm, $h = 5$ mm and $p = 0.5$ MPa. The conventional creep–damage material model of Kachanov–Rabotnov–Hayhurst (e.g. Leckie and Hayhurst, 1977; Rabotnov, 1969) has been used

$$\dot{\epsilon}_{ij}^{cr} = \frac{3}{2} a \left(\frac{\sigma_{vM}}{1 - \omega} \right)^n \frac{s_{ij}}{\sigma_{vM}} \quad \dot{\omega} = b \frac{[\alpha \sigma_I + (1 - \alpha) \sigma_{vM}]^k}{(1 - \omega)^l} \quad (1)$$

In this notation $\dot{\epsilon}_{ij}^{cr}$ are the components of the creep strain rate tensor, s_{ij} are the components of the stress deviator, σ_{vM} is the von Mises stress, σ_I is the maximum positive principal stress and ω is the damage parameter. The material constants are taken for the 316 stainless steel from Liu et al. (1994): $a = 2.13 \cdot 10^{-13}$ MPa $^{-n}/h$, $b = 9 \cdot 10^{-10}$ MPa $^{-k}/h$, $n = 3.5$, $k = 2.8$, $l = 2.8$, $\alpha = 1$. The isotropic elasticity without influence of damage has been assumed with $E = 1.44 \cdot 10^5$ MPa as Young's modulus and $\nu = 0.314$ as Poisson's ratio.

Let us start with the creep damage analysis employing the first type of boundary conditions, presented in Figure 1, a), where both edge cross sections are assumed to be movable in the axial direction as rigid bodies without rotations. The analysis has been performed using the ANSYS finite element code after incorporating the material model (1) with the help of the user defined creep material subroutine. In Altenbach et al. (2000a) we discussed various examples for beams and plates in bending, which verify the modified subroutine. Two types of finite elements available in the ANSYS code for plasticity and creep analysis were used: the 8 nodes solid element SOLID 45 and the 4 nodes shell element SHELL 43, ANSYS User's Manual Volume I – IV (1994). 30×24 elements were used for a quarter of the pipe bend in the case of the shell model and $30 \times 24 \times 4$ elements in the case of the solid model. The meshes have been justified based on the elasticity solutions and the steady state creep solutions neglecting damage. With these meshes the reference stress distributions as well as distributions of the von Mises stresses in the steady creep state were approximately the same for both solid and shell elements and did not change by further remeshing. For details of time integration and equilibrium iteration methods used in ANSYS for creep calculations we refer to ANSYS User's Manual Volume I – IV (1994) and Zienkiewicz and Taylor (1991). The time step based calculations were performed up to $\omega = \omega_* = 0.9$, where ω_* is the critical value of the damage parameter. The final distributions of the damage parameter are shown on Figure 2. According to the two finite element models the critical damage state occurs on the inner surface of the pipe bend. The solid model yields the maximum damage at the edge of the pipe bend, Figure 2, a). The shell model predicts two other zones of maximum damage, Figure 2, b). The first zone is observable on some distance from the edge. The second zone appears in the middle of the pipe bend along the circumferential coordinate. These damage distributions correspond to the dominating bending stresses in the edge zones. Figure 3, a) shows the time variations of the first principal stress in a Gauss point where the critical damage state occurs according to the solid model. Significant differences between the time variations corresponding to two types of elements are observable. In the case of the solid element based solution the first principal stress increases during the transient stage and relaxes down with the damage evolution, the shell model yields a slight change of the first principal stress during the whole creep process. The damage evolution for the given material is influenced by the first positive principal stress, if $\alpha \neq 0$ in equations (1). With the σ_I –dependence the stress state effect of the damage evolution is considered. If different

damage rates are induced by tensile and compressive stresses, the behaviour of "compressive layers" across the shell thickness is controlled by the steady state creep rate without significant damage, whereas the "tensile layers" exhibit an increasing strain rate due to damage evolution. The nonsymmetric strain distribution in the thickness direction may be the cause of errors arising by use the shell elements.

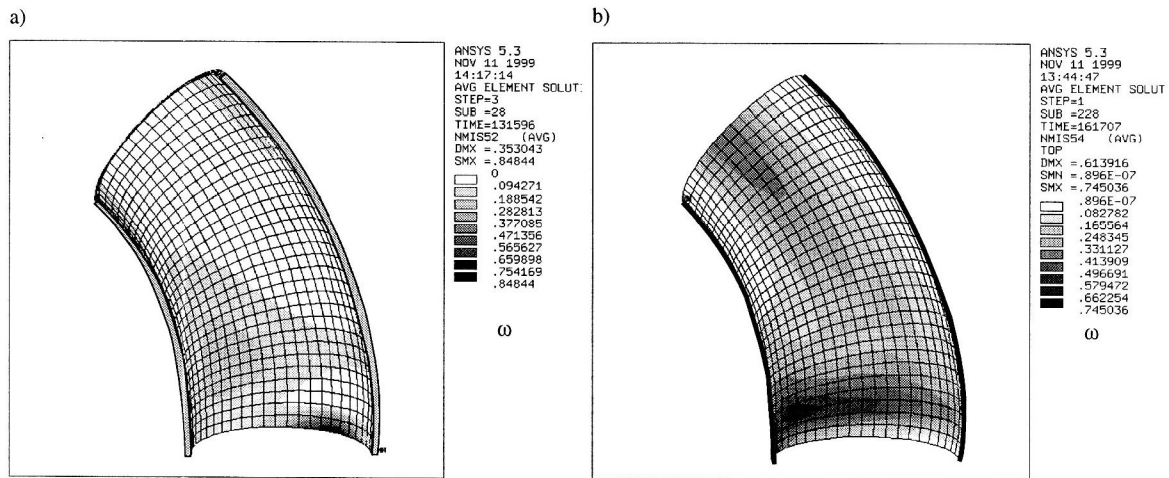


Figure 2. Distributions of the Damage Parameter at Final Time Steps, $\alpha = 1$ in Equations (1), Boundary Conditions of Type I: a) SOLID 45, b) SHELL 43

In the next example we simplify the material model excluding the stress state dependence of the damage evolution setting $\alpha = 0$ in equations (1). This leads to σ_{vM} -controlled damage. The numerical results obtained by this simplified assumption are presented on Figures 3, b) and 4. Figure 3, b) presents the time variations of the von Mises stress. Comparing with the results of the previous example, Figure 3, a), a better agreement between the time variations according to the solid and the shell models can be established. The shape of the stress relaxation curves becomes similar. Furthermore the damage distributions, Figure 4, become similar. The solid and the shell

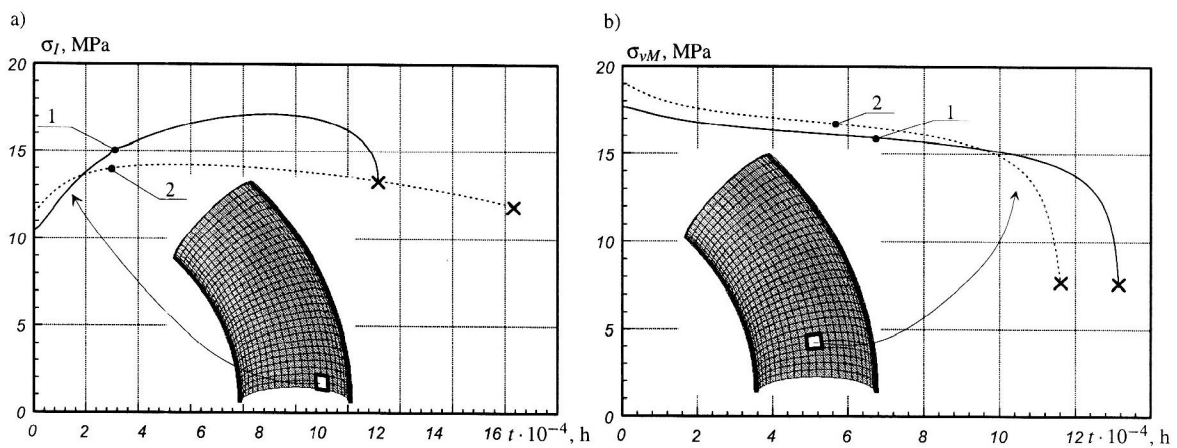


Figure 3. Time Variations: a) First Principal Stress $\alpha = 0$ in Equations (1), b) von Mises Stress $\alpha = 1$ in Equations (1), Boundary Conditions of Type I, 1 – SOLID 45, 2– SHELL 43

elements provide the same zones of the maximum damage.

In the last example we considered the σ_I -controlled damage, but simplified the boundary conditions allowing an additional rigid rotation of the pipe bend edge, Figure 1, b). According to the results of simulations the damage occurs on the outer surface along the outer bend radius, Figure 5. This is the consequence of the membrane stresses on the curved part, the influence of the bending stresses on the pipe bend edge zones is small. The solid and the shell models provide the same damage distributions.

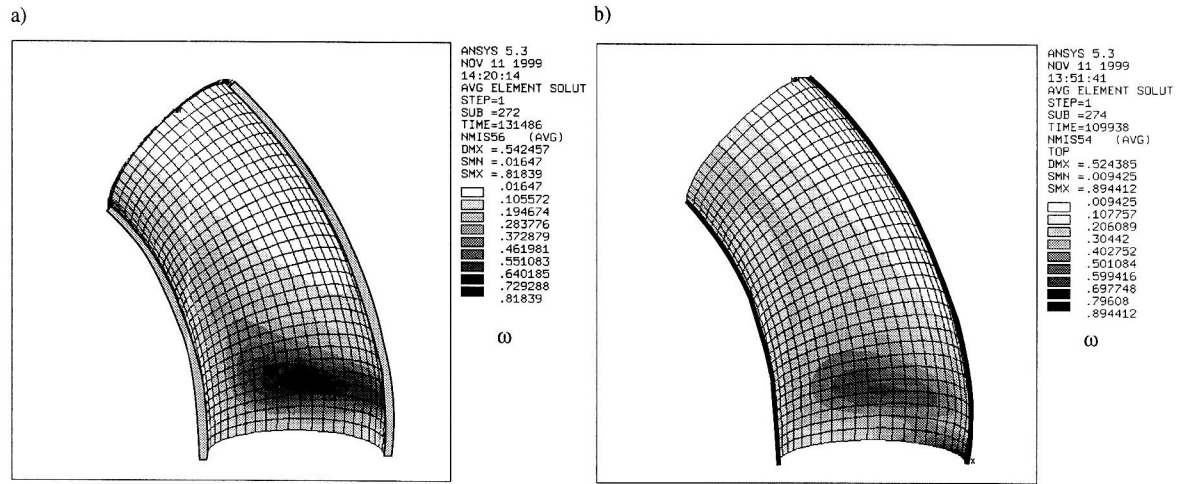


Figure 4. Distributions of the Damage Parameter at Final Time Steps, $\alpha = 0$ in Equations (1), Boundary Conditions of Type I: a) SOLID 45, b) SHELL 43

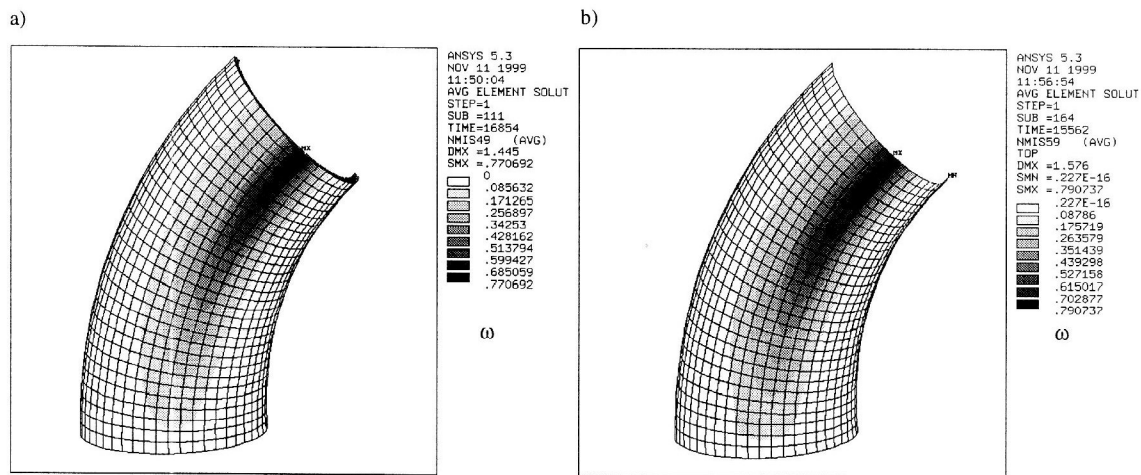


Figure 5. Distributions of the Damage Parameter at Final Time Steps, $\alpha = 1$ in Equations (1), Boundary Conditions of Type II: a) SOLID 45, b) SHELL 43

3 Material Behaviour and Cross-Section Assumptions

Creep behaviour of polycrystalline metals and alloys is a complex phenomenon accompanied by different microstructural changes. It is known from material science that for moderate stresses (below the yield limit) and elevated temperatures above $0.4T_m$ with T_m as the melting point, the steady state creep process is controlled by the climb plus glide dislocation mechanism (e.g. Nabarro and de Villiers, 1995; Riedel, 1987). The strain rate can be predicted using the power law stress function. For multiaxial stress states the deviatoric stress components and the von Mises equivalent stress are responsible for the deformation process. In addition to irreversible strain, material deterioration processes occur and lead to accelerated creep in the tertiary stage and to the final fracture. For polycrystalline materials the tertiary creep is accompanied by nucleation and growth of cavities on grain boundaries. The cavities may nucleate earlier during the creep process, possibly at primary creep stage or even by spontaneous deformation. The initially existing microdefects have negligible influence on the strain rate. As their number and size increase with time, they weaken the material providing the decrease in the load-bearing cross section. The nucleation kinetics can be related to the local grain boundary deformation as well as to the stress state characterized by the first positive principal stress (maximum tensile stress) and the von Mises stress Perrin and Hayhurst (1994). The coalescence of cavities lead to propagation of oriented microcracks and to the final fracture. Further the damage evolution induces anisotropic creep response. The cavities and microcracks nucleate on grain boundaries having different orientations. The significant influence of the damage anisotropy can be observed on the last stage before the creep rupture. Figure 6 illustrates schematically the macroscopic creep response under constant

stress and temperature. According to the discussed mechanisms the primary and secondary creep rates are domi-

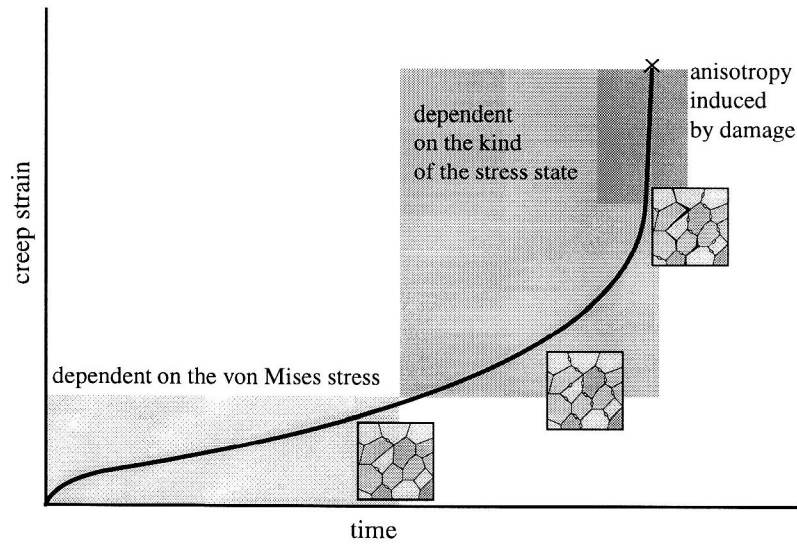


Figure 6. Typical Creep Strain Versus Time Curve

nantly controlled by the von Mises stress. The accelerated creep is additionally influenced by the kind of the stress state. For example, different tertiary creep rates and fracture times can be obtained from creep tests performed under uniaxial tension with the stress σ and under torsion with the shear stress $\sqrt{3}\tau = \sigma$ (e.g. Kowalewski, 1996). Figure 7, a) shows creep curves for tensile, compressive and shearing stresses simulated by the constitutive model (1) with material constants introduced in the previous section. The corresponding stress values provide the same value of the von Mises stress. It is obvious that the tertiary creep rate is significantly dependent on the kind of loading. Figure 7, b) presents creep curves calculated by the combined action of the normal and shear stresses. It is seen that even the small supposed shear stress can significantly influence the axial strain response and decrease the fracture time. On the other hand, if we consider the combination of the compression and shear, the shear creep strain rate remains constant. The change of the sign of the normal stress influences both the normal and shear creep responses. The stress states with combined normal tensile (compressive) stress and the small shear stress are typical for the transversely loaded beams, plates and shells.

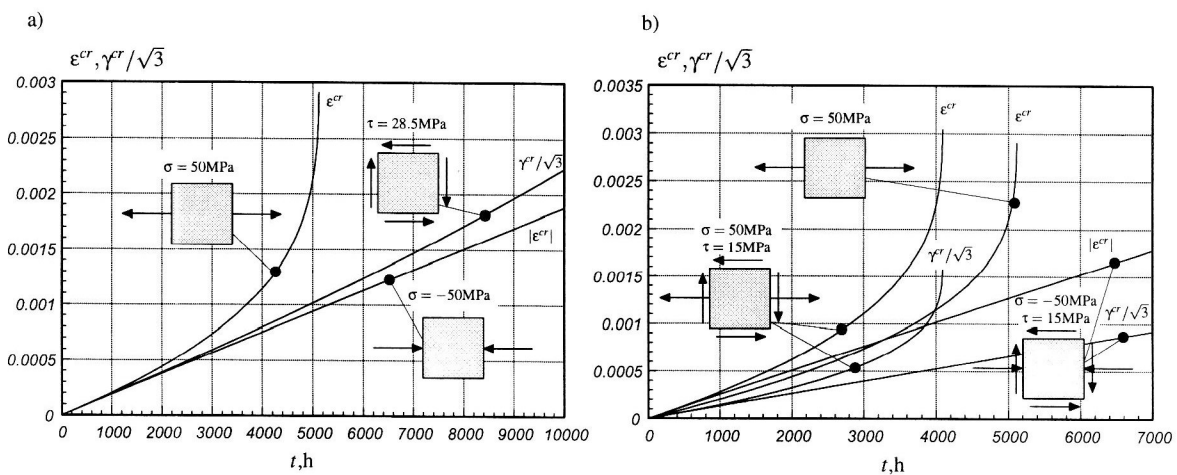


Figure 7. Creep Responses for Various Stress States Computed Using Equations (1): a) Responses by Tension, Torsion and Compression, b) Responses by Combined Tension (Compression) and Torsion

Based on the creep damage material response let us discuss the requirements regarding the through-the-thickness assumptions for modelling of thinwalled structures. First, since even the small shear stress can significantly influence the material response, the transverse shear stress and the resulting transverse shear strain cannot be neglected. Thus at least the first order shear deformation model has to be used for the creep damage analysis. Second, the dependence of the creep response on the sign of the normal stress can lead to the non-symmetrical

thickness distributions of the displacement, strain and stress fields. This has to be considered by specifying the through-the-thickness approximations for displacements or stresses.

4 Observations on Beam Equations

In what follows we discuss the assumptions of the first order shear deformation theory in detail and introduce the beam equations. The following simplified derivations will provide conclusions regarding cross section assumptions in connection with the effect of the creep damage. Let us consider a beam with a rectangular cross section, Figure 8. Considering the beam as a plane stress problem the principle of virtual displacements yields

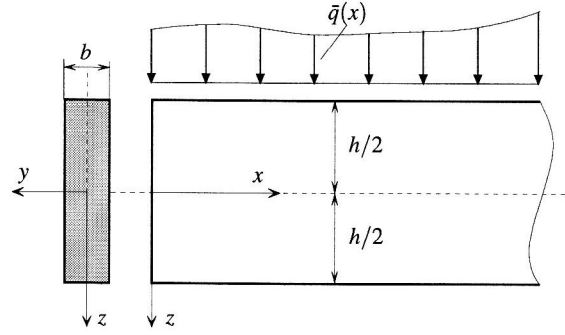


Figure 8. Straight Beam with a Rectangular Cross Section in Cartesian Coordinates

$$\frac{bh}{2} \int_0^l \int_{-1}^1 (\sigma_x \delta \varepsilon_x + \tau_{xz} \delta \gamma_{xz} + \sigma_z \delta \varepsilon_z) d\zeta dx = \int_0^l \bar{q}(x) \delta w(x, -h/2) dx \quad - \delta W_i = \delta W_a \quad (2)$$

Here l denotes the beam length, $\sigma_x, \sigma_y, \tau_{xz}$ and $\varepsilon_x, \varepsilon_y, \gamma_{xz}$ are the components of the stress and strain tensors, respectively, w is the beam deflection and $\zeta = 2z/h$ is the thickness coordinate. Here and in the following derivations we use the abbreviations

$$\frac{\partial}{\partial x}(\dots) \equiv (\dots)_{,x} \quad \frac{\partial}{\partial z}(\dots) \equiv (\dots)_{,z} \quad \frac{d}{dx}(\dots) \equiv (\dots)' \quad \frac{d}{d\zeta}(\dots) \equiv (\dots)^\bullet \quad \frac{d}{dt}(\dots) \equiv (\dots)$$

For the sake of simplicity we assume the absence of tractions on the edges $x = 0$ and $x = l$. Specifying the through-the-thickness approximations of axial displacement u and deflection w , various engineering displacement based beam theories can be obtained, Reddy et al. (1997). For example, a refined displacement based beam model can be obtained with

$$u(x, \zeta) = u_0(x) + \varphi(x) \frac{h}{2} \zeta + u_1(x) \Phi(\zeta) \quad w(x, \zeta) = w_0(x) + w_1(x) \Omega(\zeta) \quad (3)$$

where u_0 and w_0 are the displacements of the beam centerline, φ is the cross section rotation, $\Phi(\zeta)$ and $\Omega(\zeta)$ are distribution functions, which should be specified, and $u_1(x)$ and $w_1(x)$ are unknown functions of the x -coordinate.

Another possibility is the use of stress based approximations, for example, following from the elasticity solution of the Bernoulli–Euler beam equations

$$\sigma_x = \frac{6M(x)}{bh^2} \zeta \quad \tau_{xz} = \frac{3Q(x)}{2bh} (1 - \zeta^2) \quad \sigma_z = \frac{3\bar{q}(x)}{4b} \left(-\frac{2}{3} + \zeta - \frac{1}{3} \zeta^3 \right) \quad (4)$$

where Q and M are the shear force and the bending moment, respectively. Applying the stress approximations, Reissner (1950) derived the elasticity plate equations by means of the mixed variational equation. The displacement approximations (3) neglecting the terms $u_1 \Phi$ and $w_1 \Omega$ or the stress approximations (4) lead to the first order shear deformation beam theory. By generalisation the corresponding models of plates and shells can be obtained. The stress approximations (4) are not suitable for creep problems because even for the steady state creep solution of a beam the normal stress σ_x is non-linearly distributed along the thickness coordinate, Odqvist and Hult (1962).

Let us derive the first order shear deformation beam equations without assumptions for the stress σ_x . The transverse shear and the transverse normal stresses are then approximated as follows

$$\tau_{xz} = \frac{2Q(x)}{bh} \frac{\psi^\bullet(\zeta)}{\psi_0} \quad \sigma_z = \frac{\bar{q}(x)}{b} \frac{\psi(\zeta) - \psi(1)}{\psi_0} \quad \psi_0 = \psi(1) - \psi(-1) \quad (5)$$

$\psi(\zeta)$ is a given function satisfying the boundary conditions $\psi^\bullet(\pm 1) = 0$. The variation of the work of the internal forces W_i in equation (2) can be written as

$$-\delta W_i = \frac{bh}{2} \int_0^l \int_{-1}^1 \delta(\tau_{xz}\gamma_{xz} + \sigma_z \varepsilon_z) - \underline{(\gamma_{xz}\delta\tau_{xz} + \varepsilon_z\delta\sigma_z - \sigma_x\delta\varepsilon_x)} d\zeta dx \quad (6)$$

With the approximations (5) and the linear strain–displacement equations $\varepsilon_x = u_{,x}$, $\varepsilon_z = w_{,z}$, and $\gamma_{xz} = u_{,z} + w_{,x}$ we obtain

$$\frac{bh}{2} \int_0^l \int_{-1}^1 \delta(\tau_{xz}\gamma_{xz} + \sigma_z \varepsilon_z) d\zeta dx = \int_0^l [\delta(Q\tilde{w}' - Q\tilde{u}) + \bar{q}\delta w(x, -1) - \bar{q}\tilde{w}] dx \quad (7)$$

with

$$\tilde{w}(x) = \frac{1}{\psi_0} \int_{-1}^1 w(x, \zeta) \psi^\bullet(\zeta) d\zeta \quad \tilde{u}(x) = \frac{2}{h} \frac{1}{\psi_0} \int_{-1}^1 u(x, \zeta) \psi^{\bullet\bullet}(\zeta) d\zeta, \quad (8)$$

Let us assume the additive split of the total strain tensor into an elastic and a creep part $\varepsilon_{ij} = \varepsilon_{ij}^{el} + \varepsilon_{ij}^{cr}$, and ε_{ij}^{cr} to be known functions of the coordinates x, ζ for the fixed time variable. Further we will use the linear through-the-thickness approximation of the axial displacement $u(x, \zeta) = u_0(x) + \zeta\varphi(x)h/2$. With these assumptions the underlined term in equation (6) can be transformed into

$$\int_0^l \left[N' \delta u_0 + M' \delta \varphi + \frac{1}{Gbhk} Q \delta Q + \tilde{\gamma}^{cr} \delta Q \right] dx \quad (9)$$

with the shear modulus G and

$$N(x) = \frac{bh}{2} \int_{-1}^1 \sigma_x(x, \zeta) d\zeta \quad M(x) = \frac{bh^2}{4} \int_{-1}^1 \sigma_x(x, \zeta) \zeta d\zeta \quad (10)$$

$$\frac{1}{k} = \frac{2}{\psi_0^2} \int_{-1}^1 \psi^{\bullet\bullet}(\zeta) d\zeta \quad \tilde{\gamma}^{cr}(x) = \frac{1}{\psi_0} \int_{-1}^1 \gamma_{xz}^{cr}(x, \zeta) \psi^\bullet(\zeta) d\zeta \quad (11)$$

After summing all terms in equation (2) we obtain the following variational equation

$$\int_0^l \left[(Q - M') \delta \varphi - (Q' + \bar{q}) \delta \tilde{w} - N' \delta u_0 + \left(\varphi + \tilde{w}' - \frac{1}{Gbhk} Q - \tilde{\gamma}^{cr} \right) \delta Q \right] dx = 0 \quad (12)$$

Assuming the variations of the functions u_0 , φ , \tilde{w} and Q to be independent equation (12) provides the following ordinary differential equations

$$N' = 0 \quad M' - Q = 0 \quad Q' + \bar{q} = 0 \quad Q = Gbhk(\varphi + \tilde{w}' - \tilde{\gamma}^{cr}) \quad (13)$$

The first three equations are the classical equilibrium conditions of the beam. The last equation is the constitutive equation connecting the shear force and the averaged shear strain. From this equation and with the assumed linear

through-the-thickness approximation of the axial displacement we obtain

$$u(x, \zeta) = u_0(x) - \zeta \frac{h}{2} w'(x) + \zeta \frac{h}{2} \frac{Q(x)}{Gbhk} + \zeta \frac{h}{2} \tilde{\gamma}^{cr}(x)$$

The second term is the rotation of the normal to the centerline (Bernoulli's hypothesis), the third term denotes the influence of the shear force in the sense of the Timoshenko theory and the last term is the contribution of the averaged creep shear strain. The coefficient k and the average of the creep strain $\tilde{\gamma}^{cr}$ are unknown while the function $\psi^*(\zeta)$ is not specified. The parabolic shear stress distribution function according to the solution of the elastic Bernoulli beam $\psi^*(\zeta) = 1 - \zeta^2$ yields the classical shear correction factor $k = 5/6$ for a homogeneous rectangular cross section. Let us consider the classical steady state creep solution of a Bernoulli beam (e.g. Odqvist and Hult, 1962). Assuming the Norton-Bailey creep law we obtain

$$\dot{\epsilon}_x \approx \dot{\epsilon}_x^{cr} = a\sigma_x^n = -w''\zeta \frac{h}{2}$$

The stress σ_x can be expressed as

$$\sigma_x(x, \zeta) = \left(-\frac{w''^{1/n}}{a} \right) |\zeta|^{(1/n)-1} \zeta \left(\frac{h}{2} \right)^{1/n} = \frac{M(x)}{\alpha bh^2} |\zeta|^{(1/n)-1} \zeta \quad \alpha = \frac{n}{2(2n+1)}$$

After inserting this equation into the equilibrium condition

$$\sigma_{x,x} + \frac{2}{h} \tau_{xz,\zeta} = 0 \quad (14)$$

and the integration with respect to the ζ coordinate, the distribution function can be obtained as

$$\psi^*(\zeta) = 1 - \zeta^2 |\zeta|^{(1/n)-1} \quad (15)$$

Inserting this function into the first equation (11) we obtain $k = (3n+2)/(4n+2)$. Setting $n = 1$ this equation yields the shear correction factor of elastic beam with rectangular cross section. Since the value of n varies between 3 and 10 for metallic materials we can estimate, for example, if $n = 3; 10$, $k = 11/14; 16/21$ respectively. It can be seen that k in the case of steady state creep is influenced by the creep exponent. The value of k decreases with increasing creep exponent (for $n \rightarrow \infty$ we obtain $k_\infty = 3/4$) and consequently with increasing creep strain rate. Because the effect of damage is connected with the increase of the creep strain rate, the decreasing of the shear correction coefficient can be expected if damage evolution is taken into account. In addition, if the damage rate differs for tensile and compressive stresses, the thickness distribution of the transverse shear stress will be non-symmetrical. In this case the function ψ^* cannot be selected a-priori.

5 Numerical Estimations

In order to solve the creep problem for a beam numerically we formulate the variational problem with u_0 , φ and Q as principal unknowns for a fixed time variable. First we specify the function of the transverse shear stress distribution as $\psi^*(\zeta) = 1 - \zeta^2$. Assuming that the shear force Q satisfies the equilibrium condition $Q' = -\bar{q}$ and the static boundary conditions (if prescribed) at the beam edges, and the functions u_0 and φ satisfy the kinematic boundary conditions, the variational equation (12) can be transformed into

$$\int_0^l \left[N' \delta u_0 + M \delta \varphi' + \left(\varphi - \frac{1}{Gbhk} Q - \tilde{\gamma}^{cr} \right) \delta Q + Q \delta \varphi \right] dx = 0 \quad (16)$$

From Hooke's law and the assumed approximations follows

$$\begin{aligned} \sigma_x(x, \zeta) &= E \left[u_0'(x) + \zeta \frac{h}{2} \varphi'(x) - \epsilon_x^{cr}(x, \zeta) \right] + \nu \sigma_z(x, \zeta) \\ \epsilon_z(x, \zeta) &= \frac{1-\nu^2}{E} \sigma_z(x, \zeta) - \nu \left[u_0'(x) + \zeta \frac{h}{2} \varphi'(x) \right] + \nu \epsilon_x^{cr}(x, \zeta) + \epsilon_z^{cr}(x, \zeta) \end{aligned} \quad (17)$$

whereas σ_z is determined according to equations (5). Inserting the normal stress σ_x into the equations defining the stress resultants (10) we obtain

$$\begin{aligned} N(x) &= EAu'_0(x) + a_N h v \bar{q}(x) - N^{cr}(x) & M(x) &= EI\phi'_0(x) + a_M h^2 v \bar{q}(x) - M^{cr}(x) \\ a_N &= \frac{1}{2} \int_{-1}^1 \frac{\Psi(\zeta) - \Psi(1)}{\Psi_0} d\zeta & a_M &= \frac{1}{4} \int_{-1}^1 \frac{\Psi(\zeta) - \Psi(1)}{\Psi_0} \zeta d\zeta \\ N^{cr}(x) &= E \frac{bh}{2} \int_{-1}^1 \varepsilon_x^{cr}(x, \zeta) d\zeta & M^{cr}(x) &= E \frac{bh^2}{4} \int_{-1}^1 \varepsilon_x^{cr}(x, \zeta) \zeta d\zeta \end{aligned} \quad (18)$$

where $A = bh$ and $I = bh^3/12$ for the rectangular cross section. Assuming that $\varepsilon_x^{cr}(x, \zeta)$ and $\bar{\gamma}^{cr}(x)$ are known functions for a fixed time variable, the equation (16) can be written as follows

$$\delta \int_0^l \left[\frac{EA}{2} u_0'^2 + \frac{EI}{2} \phi_0'^2 - \frac{1}{2GAk} Q^2 + Q\phi + v\bar{q}h(a_N u_0' + h a_M \phi') - M^{cr} \phi' - N^{cr} u_0' - \bar{\gamma}^{cr} Q \right] dx = \delta \Pi = 0 \quad (19)$$

Let us assume that the beam is uniformly loaded and $\bar{q}(x) = q_0$. Then the shear force can be specified as $Q(x) = Q_0 - q_0 x$, with Q_0 as an unknown reaction force at the edge $x = 0$. Further we can specify the unknown functions u_0 and ϕ as follows

$$u_0(x) = \frac{1}{EA} \mathbf{S}_u^T(x) \mathbf{a}_u \quad \phi(x) = \frac{1}{EI} \mathbf{S}_\phi^T(x) \mathbf{a}_\phi$$

where $\mathbf{S}_u(x)$ and $\mathbf{S}_\phi(x)$ are the vectors of trial functions and \mathbf{a}_u and \mathbf{a}_ϕ are the vectors of unknown coefficients. Applying the Ritz method we obtain from the conditions $\Pi_{,\mathbf{a}_u} = 0$, $\Pi_{,\mathbf{a}_\phi} = 0$ and $\Pi_{,Q_0} = 0$ the following set of linear algebraic equations

$$\begin{aligned} \int_0^l \mathbf{S}_u^T(x) \mathbf{S}'_u(x) dx \mathbf{a}_u &= -v q_0 h a_N [\mathbf{S}_u(l) - \mathbf{S}_u(0)] + \int_0^l N^{cr}(x) \mathbf{S}'_u(x) dx \\ \int_0^l \mathbf{S}_\phi^T(x) \mathbf{S}'_\phi(x) dx \mathbf{a}_\phi + Q_0 \int_0^l \mathbf{S}_\phi(x) dx &= -v q_0 h^2 a_M [\mathbf{S}_\phi(l) - \mathbf{S}_\phi(0)] + \int_0^l M^{cr}(x) \mathbf{S}'_\phi(x) dx \\ Q_0 &= \frac{ql}{2} + \frac{GAk}{l} \left(\frac{1}{EI} \int_0^l \mathbf{S}_\phi^T(x) dx \mathbf{a}_\phi - \int_0^l \bar{\gamma}^{cr}(x) dx \right) \end{aligned} \quad (20)$$

For statically determinate beams the last equation in (20) is identically satisfied. The solution provides the three unknown functions u_0 , ϕ and Q at the current time step. Then the normal stress σ_x follows from the first equation in (17). By some transformations this equation can be formulated in terms of the stress resultants

$$\sigma_x(x, \zeta) = \frac{1}{A} [N(x) + N^{cr}(x)] + \zeta \frac{h}{2I} [M(x) + M^{cr}(x)] - E \varepsilon_x^{cr}(x, \zeta) + v \sigma_z(x, \zeta) \quad (21)$$

After inserting this equation into the equilibrium condition (14) and integration with respect to the ζ coordinate we obtain the transverse shear stress as follows

$$\tau_{xz}(x, \zeta) = \frac{h^2}{8I} (1 - \zeta^2) [Q(x) + M^{cr'}(x)] - \frac{h}{2A} (\zeta + 1) N^{cr'}(x) + \frac{Eh}{2} \int_{-1}^{\zeta} \varepsilon_x^{cr}(x, \zeta) d\zeta \quad (22)$$

The obtained expression does not correspond to the assumed single term approximation of the transverse shear stress (5). Since the function $Q(x)$ is known, we can minimize the residual

$$\int_0^l \left[\tau_{xz}(x, \zeta) - \frac{2Q(x)}{A} \frac{\Psi^*(\zeta)}{\Psi_0} \right] Q(x) dx = 0 \quad (23)$$

From this equation we obtain

$$\frac{\Psi^*(\zeta)}{\Psi_0} = \frac{3}{4}(1+a_1)(1-\zeta^2) - a_2(1+\zeta) + \int_{-1}^{\zeta} f^{cr}(\zeta)d\zeta \quad (24)$$

with

$$a_1 = \frac{[M^{cr}(x)Q(x)]_{x=0}^{x=l} + q_0 \int_0^l M^{cr}(x)dx}{\int_0^l Q^2(x)dx} \quad a_2 = \frac{h}{4} \frac{[N^{cr}(x)Q(x)]_{x=0}^{x=l} + q_0 \int_0^l N^{cr}(x)dx}{\int_0^l Q^2(x)dx}$$

$$f^{cr}(\zeta) = \frac{Ebh^2}{4} \frac{[\varepsilon^{cr}(x, \zeta)Q(x)]_{x=0}^{x=l} + q_0 \int_0^l \varepsilon^{cr}(x, \zeta)dx}{\int_0^l Q^2(x)dx}$$

The computed function $\Psi^*(\zeta)$ provides the shear correction factor k and the averaged shear strain $\bar{\gamma}^{cr}$, equations (11). Then the functions depending on the x coordinate must be recalculated at the current time step according to the equation (20). The iteration cycle can be repeated until the value of k reaches the desired accuracy. For the known stresses and the damage parameter at the current time step the constitutive model (1) yields the rates of creep strain and damage. From these the new values for time $t + \Delta t$ can be computed using the implicit time integration procedure

$$\varepsilon_{ij}^{cr}(x, \zeta, t + \Delta t) = \varepsilon_{ij}^{cr}(x, \zeta, t) + \Delta t[(1 - \theta)\dot{\varepsilon}_{ij}^{cr}(x, \zeta, t) + \theta\dot{\varepsilon}_{ij}^{cr}(x, \zeta, t + \Delta t)]$$

$$\omega(x, \zeta, t + \Delta t) = \omega(x, \zeta, t) + \Delta t[(1 - \theta)\dot{\omega}(x, \zeta, t) + \theta\dot{\omega}(x, \zeta, t + \Delta t)]$$

$$\varepsilon_{ij}^{cr}(x, \zeta, 0) = 0 \quad \omega(x, \zeta, 0) = 0 \quad \omega(x, \zeta, t) < \omega_*$$

Details of the Ritz method and the time step procedure are presented in Altenbach et al. (2000a) and Naumenko (1996).

Figure 9 presents the simulation results for the uniformly loaded beam with clamped edges. For the calculations we set $l = 1000\text{mm}$, $b = 50\text{mm}$, $h = 100\text{mm}$ and $q_0 = 50\text{N/mm}$ with l as the beam length. The material model is

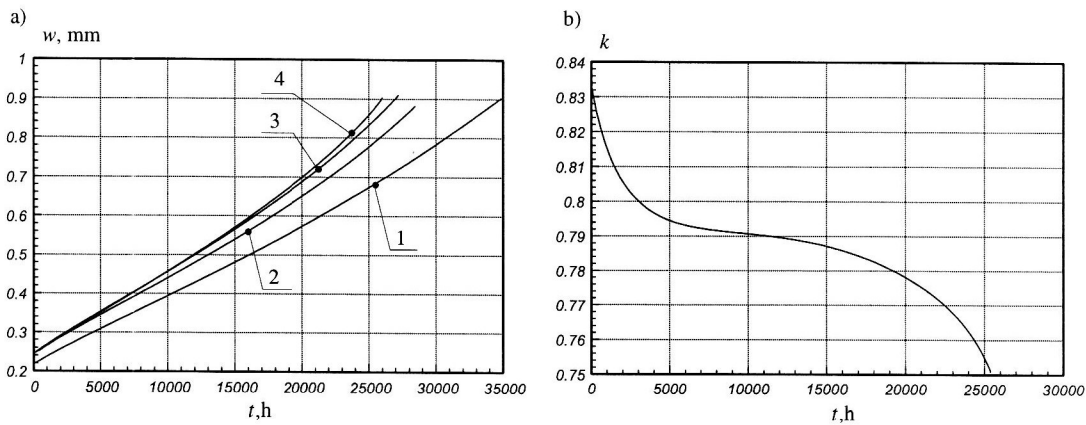


Figure 9. Time Dependent Solutions of a Clamped Beam a) Maximum Deflection vs. Time, b) Shear Correction Factor vs. Time, 1 – Bernoulli–Euler Beam Theory, 2 – First Order Shear Deformation Theory with Parabolic Shear Stress Distribution, 3 – First Order Shear Deformation Theory with Modified Shear Stress, 4 – Solution Using the ANSYS Code with PLANE 42 Elements

the same as that used for the pipe bend analysis. The curve 1 on the Figure 9, a) is the time dependent maximum deflection calculated by use of the Bernoulli–Euler beam theory. The corresponding equations and the numerical procedure are presented in Altenbach et al. (2000a). The curve 2 is obtained using the beam model with the parabolic transverse shear stress according to equations (4) and the shear correction coefficient as $5/6$. The curve

3 is the solution based on the equations discussed above with modified transverse shear stress. The curve 4 is the ANSYS code finite element solution obtained with plane elements PLANE 42. It is obvious that the Bernoulli–Euler beam theory cannot adequately predict the deflection growth. Further, the first order shear deformation theory underestimates the deflection particularly on the last stage of the creep process. By modification of the transverse shear stress distribution function a better agreement between the elementary beam theory and the plane stress solution is obtained. Figure 9, b) presents the dependence on time of the shear correction factor. With decreasing value of k we can conclude that the influence of the shear correction terms in discussed equations increases.

The results for the beam show that the modified shear stress influences the deflection growth in the creep–damage process. On the other hand if we neglect the damage evolution, the steady state creep solution provides the shear stress distribution close to the parabolic one, equation (15). From the beam equations we can conclude that the standard first order shear deformation theory can be applied for the creep analysis if damage effects are negligible. If damage evolution induces the stress state dependent material response, the transverse shear stress distribution becomes significant. The average of the transverse shear creep strain and the shear correction factor contribute to the time–dependent solution.

Let us emphasize that in the case of plates and shells the shear correction factor is additionally responsible for the boundary layer stress distributions. The boundary layer solutions are known from the closed form solutions of the elasticity plate equations (e.g. Reissner, 1990). In the case of creep this kind of the solution is important for the time dependent stress redistributions. As we observed in the pipe bend analysis the solutions based on the shell and solid models disagree if the stress state dependent damage evolution is taken into account. Particularly both the models provide different edge zone stress redistributions. Additional plots of illustrating boundary layer effects for the pipe bend in the elasticity and creep solutions are presented in Altenbach et al. (2000b)

6 Conclusions

We discussed non–linear time–dependent solutions based on the first order shear deformation equations of beams, plates and shells in connection with creep–damage material models. The finite element analysis of the pipe bend has been performed with solid and shell type finite elements available in the ANSYS code. The results agree in the case of the linear elastic material behaviour as well as the creep behaviour controlled by the von Mises stress. If the damage evolution is taken into account the shell and the solid models lead to different predictions. Particularly, the disagreement is observed on the edge zone stress redistributions. This is explained to be the result of the dependence of the creep response on the kind of the stress state induced by damage evolution. The transverse shear stress and the transverse normal stress can essentially influence the deformation behaviour if time–dependent creep and damage are taken into account. These stresses cannot be accurately computed within the framework of the first order shear deformation theory. On the beam equations we demonstrated that the shear correction factor and the function of the thickness distribution of the transverse shear stress have to be modified by solving the creep–damage problems.

Further investigations should be directed to the examinations of higher order terms in through–the–thickness displacement or stress field approximations of beams, plates and shells in connection with creep damage studies. Particularly the higher order theories should be discussed with respect to the accuracy of edge zone time–dependent stress redistributions for various types of boundary conditions.

Acknowledgement

I gratefully acknowledge the support of the German Research Foundation (DFG) under Grant GRK 203 for funding my research work in the Graduiertenkolleg "Modellierung, Berechnung und Identifikation mechanischer Systeme". Further I acknowledge the help from Dr.-Ing. V. Kushnevsky and Dr.-Ing. H. Chunxiao in finite–element simulations with ANSYS code.

Literature

1. Altenbach, H.; Altenbach, J.; Naumenko, K.: Ebene Flächentragwerke. Berlin u.a.: Springer-Verlag, (1998).

2. Altenbach, H.; Kolarow, G.; Morachkovsky, O.; Naumenko, K.: On the accuracy of creep-damage predictions in thinwalled structures using the finite element method. *Comp. Mech.*, 25, (2000a), 87–98.
3. Altenbach, H.; Kushnevsky, V.; Naumenko, K.: On the use of solid and shell type finite elements in creep-damage predictions of thinwalled structures. *Arch. Appl. Mech.*, (2000b), in press.
4. Altenbach, H.; Morachkovsky, O.; Naumenko, K.; Sychov, A.: Geometrically nonlinear bending of thin-walled shells and plates under creep–damage conditions. *Arch. Appl. Mech.*, 67, (1997), 339–352.
5. ANSYS User's Manual Volume I – IV: Swanson Analysis Systems, Inc., (1994).
6. Betten, J.; Borrmann, M.; Butters, T.: Materialgleichungen zur Beschreibung des primären Kriechverhaltens innendruckbeanspruchter Zylinderschalen aus isotropem Werkstoff. *Ing. Arch.*, 60, 3, (1989), 99–109.
7. Bodnar, A.; Chrzanowski, M.: Cracking of creeping plates in terms of continuum damage mechanics. *Mech. Teor. i Stos.*, 32, 1, (1994), 31–41.
8. Hayhurst, D. R.: The use of continuum damage mechanics in creep analysis for design. *J. of Strain Analysis*, 25, 3, (1994), 233–241.
9. Kowalewski, Z.: Creep rupture of copper under complex stress state at elevated temperature. In: *Design and life assessment at high temperature*, pages 113 – 122, London: Mechanical Engineering Publ., (1996).
10. Leckie, F.; Hayhurst, D.: Constitutive Equations for Creep Rupture. *Acta Metall.*, 25, (1977), 1059 – 1070.
11. Liu, Y.; Murakami, S.; Kanagawa, Y.: Mesh–dependence and stress singularity in finite element analysis of creep crack growth by continuum damage mechanics approach. *Eur. J. Mech., A Solids*, 13, 3, (1994), 395–417.
12. Miyazaki, N.: Creep buckling analyses of circular cylindrical shells under axial compression – bifurcation buckling analysis by the finite element method. *Trans. of ASME. J. Press. Ves. Techn.*, 109, (1987), 179–183.
13. Nabarro, F. R. N.; de Villiers, H. L.: *The Physics of Creep. Creep and Creep-resistant Alloys*. London: Taylor & Francis, (1995).
14. Naumenko, K.: Modellierung und Berechnung der Langzeitfestigkeit dünnwandiger Flächentragwerke unter Berücksichtigung von Werkstoffkriechen und Schädigung. Dissertation, Otto-von-Guericke Universität Magdeburg, (1996).
15. Odqvist, F.; Hult, J.: *Kriechfestigkeit metallischer Werkstoffe*. Berlin u.a.: Springer, (1962).
16. Perrin, I. J.; Hayhurst, D. R.: Creep constitutive equations for a 0.5Cr-0.5Mo-0.25V ferritic steel in the temperature range 600–675°C. *J. of Strain Anal.*, 31, 4, (1994), 299–314.
17. Rabotnov, Y. N.: *Creep Problems in Structural Members*. Amsterdam: North Holland, (1969).
18. Reddy, J.; Wang, C.; Lee, K.: Relationships between bending solutions of classical and shear deformation beam theories. *Int. J. Solids. Struct.*, 34, 26, (1997), 3373–3384.
19. Reissner, E.: A variational theorem in elasticity. *J. Math. Phys.*, 29, (1950), 90–95.
20. Reissner, E.: Reflections on the theory of elastic plates. *Apl. Mech. Rev.*, 38, 11, (1985), 1453–1464.
21. Reissner, E.: A note on the boundary layer in the sixth-order theory of transverse bending of anisotropic shear-deformable elastic plates. *Comm. Appl. Num. Meth.*, 6, (1990), 519–524.
22. Riedel, H.: *Fracture at High Temperatures. Materials Research and Engineering*, Berlin et al.: Springer, (1987).
23. Takezono, S.; Fujoka, S.: The creep of moderately thick shells of revolution under axisymmetrical load. In: *Creep in Structures* (edited by Ponter, A. R. S.), pages 128–143, Berlin et al.: Springer-Verlag, (1981).
24. Zienkiewicz, O. C.; Taylor, R. L.: *The Finite Element Method*. London et al.: McGraw–Hill, (1991).

Address: Dr.-Ing. Konstantin Naumenko, Fachbereich Ingenieurwissenschaften, Lehrstuhl für Technische Mechanik, Martin-Luther-Universität Halle-Wittenberg, D-06099 Halle.
e-mail: konstantin.naumenko@iw.uni-halle.de